# De Novo Design, Synthesis, and In Vitro Evaluation of Inhibitors for Prokaryotic tRNA-Guanine Transglycosylase: A Dramatic Sulfur Effect on Binding Affinity

Emmanuel A. Meyer,[a] Ruth Brenk,[b]
Ronald K. Castellano,[a] Maya Furler,[a] Gerhard Klebe,*[b]
and François Diederich*[a]

**KEYWORDS:**

antibiotics · de novo design · enzyme inhibitors · structure–activity relationships · tRNA

Shigellosis (bacillary dysentary) is a bacterial disease that results in more than one million deaths each year.[1] Enteric infections caused by the Shigella organisms have traditionally been treated with antibiotics.[2] However, the emergence of multi-drug-resistant strains and a longstanding lack of vaccine availability demands the development of novel therapeutic strategies.[3] To this end, tRNA-guanine transglycosylase (TGT, EC 2.4.2.29) has been recognized as a key enzyme in the regulation of bacterial virulence and a target for de novo drug design, as shown by Grädler et al.[4]

TGT is involved in the biosynthesis of the highly modified nucleobase queuine (Q; Scheme 1) found in the anticodon loop of some tRNAs.[5] Prokaryotic TGT catalyzes the exchange of guanine from the anticodon loop with the queuine precursor preQ$_1$.[6, 7] Although the precise physiological role of queuine has yet to be determined, it is certainly involved in codon–anticodon interactions during translation.[8] The use of specific inhibitors to block the biological effect of TGT is expected to result in tRNAs that lack queuine in the anticodon. Inefficient translation would then interfere with virulence regulation and produce the desired bacterial apathogenicity.[9]

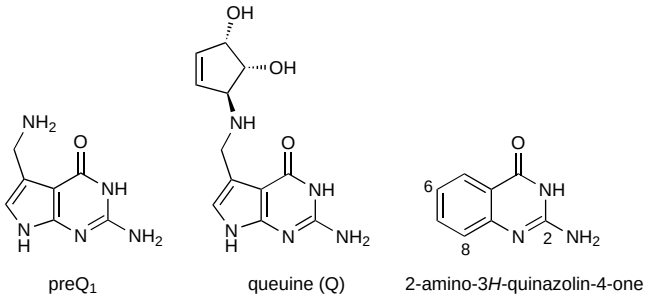


***Scheme 1.*** *Structures of TGT substrates.*

We became interested in the development of a new family of inhibitors of TGT as part of our continuing program of X-ray structure based de novo design of enzyme inhibitors and exploration of molecular recognition principles at biological receptor sites.[10, 11] We used the X-ray crystal structure of the TGT–preQ$_1$ complex of *Zymomonas mobilis*[12] and the modeling program MOLOC to visualize and analyze the substrate binding pocket[13] and thereby identified 2-amino-3*H*-quinazolin-4-one (Scheme 1) as a promising new scaffold for TGT inhibitors. This heterocycle preserves the hydrogen bonding pattern of the natural substrates guanine and preQ$_1$. Specific recognition in the active site should arise from hydrogen bonding between the C(4)=O group of the inhibitor and both the backbone NH group of Gly230 and the side chain amide NH$_2$ group of Gln203 (Scheme 2); additional hydrogen bonds should form between the carboxylate of the Asp156 residue and the N(3)–H and C(2)–NH$_2$ groups of the lead structure. The NH$_2$ group attached at position 6 is expected to interact with the C=O group of Leu231.[4] In the projected complex, the aromatic heterocycle is sandwiched between the flexible phenolic side chain of Tyr106 and the side chain of Met260.[4, 14]

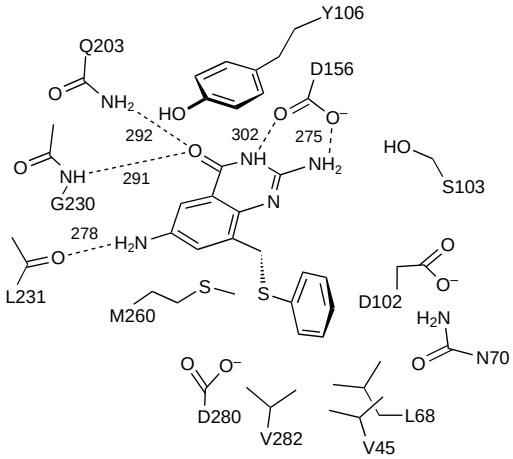


***Scheme 2.*** *Active site of TGT (Z.* mobilis*) with designed inhibitor* ***1 d****. Distances in pm.*

Grädler et al. identified the polar side chains of Asp102, Asp280, and Asn70 (Scheme 2) as targets for additional affinity- and selectivity-enhancing hydrogen-bonding contacts by using the de novo design program LUDI.[4] Our strategy exploits specific nonpolar contacts in enzyme active sites to enhance binding free energy. Our analysis indeed revealed a lipophilic pocket at the bottom of the active site, defined by Leu68, Val45, and Val282, which can accommodate residues up to the size of aromatic rings (Scheme 2). The modeling showed that side

[a] *Prof. F. Diederich, Dipl. Chem. E. A. Meyer, Dr. R. K. Castellano, M. Furler*
*Laboratorium für Organische Chemie*
*ETH-Hönggerberg, HCI, 8093 Zürich (Switzerland)*
*Fax: (+41) 1-632-1109*
*E-mail: diederich@org.chem.ethz.ch*

[b] *Prof. G. Klebe, R. Brenk*
*Institut für Pharmazeutische Chemie*
*Philipps-Universität Marburg*
*Marbacher Weg 6, 35032 Marburg (Germany)*
*Fax: (+49) 6421-282-1313*
*E-mail: klebe@mailer.uni-marburg.de*

 © WILEY-VCH-Verlag GmbH, 69451 Weinheim, Germany, 2002 1439-4227/02/03/02-03 $ 17.50+.50/0 ChemBioChem **2002**, No. 02-03

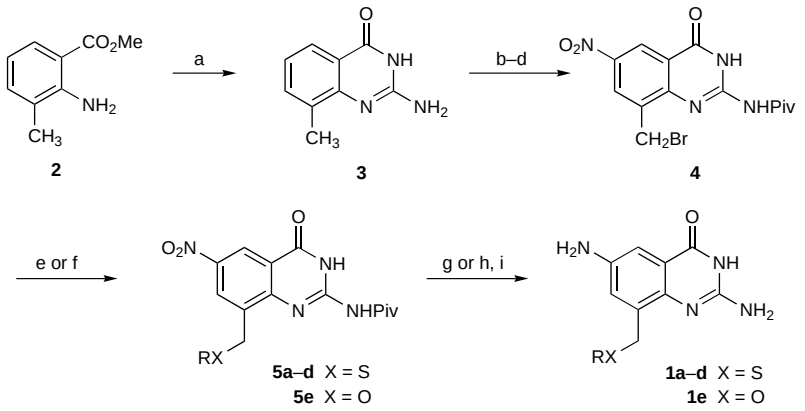


***Scheme 3.*** *Synthesis of inhibitors* ***1a–e****. Reagents and conditions: a) Chloroformamidinium hydrochloride, dimethylsulfone, 150 °C, 1 h, 98 %; b) $HNO_3$, $H_2SO_4$, 20 °C, 6 h, 72 %; c) PivCl, Py, DMA, 110 °C, 12 h, 82 %; d) NBS, $(PhCOO)_2$, $CCl_4$, Δ, 12 h, 59 %; e) RSH, nBuLi, THF, 20 °C, 3 h, 70–75 %; f) phenol, NaH, THF, 0 → 20 °C, 4 h, 52 %; g) $SnCl_2$, EtOH, 70 °C, 4 h, ca. 50 % (X = S); h) Zn, HOAc, $H_2O$, 20 °C, 3 h, 74 % (X = O); i) HCl, EtOH, 70 °C, 3 h, ca. 80 %. DMA = N,N-dimethylacetamide; NBS = N-bromosuccinimide; Py = pyridine; Piv = pivaloyl.* ***1a****: R = cyclohexyl,* ***1b****: R = 2-imidazolyl,* ***1c****: R = propyl,* ***1d****,* ***1e****: R = phenyl.*

chains attached to position 8 of the 2-aminoquinazolinone scaffold could potentially point exactly into this pocket. Therefore, we prepared a small series of inhibitors **1a–f** (Schemes 3 and 4) with diverse lipophilic residues in position 8 in order to exploit the binding free energy contributions that result when this pocket is filled. Here, we report the synthesis of these new lead compounds, which have demonstrated up to submicromolar activity, as well as the X-ray structural characterization of two of the complexes formed with TGT (*Z. mobilis*).

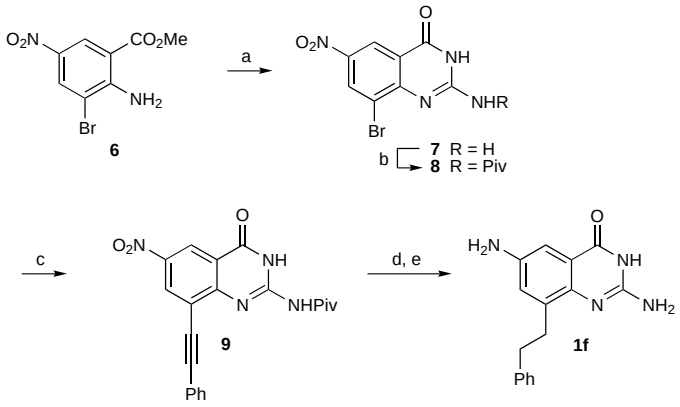


***Scheme 4.*** *Synthesis of inhibitor* ***1f****. Reagents and conditions: a) Guanidinium hydrochloride, EtONa, EtOH, Δ, 60 h, 63 %; b) PivCl, Py, DMA, 110 °C, 8 h, 71 %; c) phenylacetylene, $[Pd(OAc)_2]$, P(o-tol)$_3$, CuI, $NEt_3$, MeCN, Δ, 15 h, 23 %; d) $H_2$, Pd/C (10 %), EtOH, 70 °C, 4 h, 46 %; e) HCl, EtOH, 70 °C, 4 h, 93 %.* o-*tol* = o-*tolyl*.

Inhibitors **1a–e** (Scheme 3) were synthesised from commercially available 3-methyl-2-nitrobenzoic acid which was esterified (HCl, MeOH) to the methyl ester and subsequently hydrogenated ($H_2$, Pd/C, MeOH) to give amino ester **2** (77 %). Quinazoline **3** was formed by treatment of **2** with chloroformamidinium hydrochloride (98 %).[15] Nitration, introduction of the pivaloyl protecting group, and radical bromination furnished the bromomethyl derivative **4**. Substitution with various thiols afforded **5a–d**,[16] while reaction with phenol gave aryl ether **5e**. Reduction of the nitro group and *N*-deprotection finally provided **1a–e**.

The phenethyl derivative **1f** was prepared from 2-amino-5-nitrobenzoic acid which was transformed by esterification ($SOCl_2$, MeOH, 77 %) and bromination ($Br_2$, AcOH, 92 %) into amino ester **6** (Scheme 4). Ring closure with guanidinium hydrochloride followed by nitration furnished 2-aminoquinazolinone **7**,[17] which was protected to form compound **8** and subjected to Sonogashira cross-coupling with phenylacetylene to give **9**.[18] Hydrogenation and deprotection afforded the desired inhibitor **1f**.

The binding affinities of the target compounds **1a–f** for TGT (*Z. mobilis*) were measured by using the procedure described by Grädler et al.[4] All derivatives were highly active against TGT (Scheme 5). Thiophenyl ether **1d** showed one of the highest activities reported to date for TGT inhibitors (binding affinity for TGT, $K_i = 100$ nM).

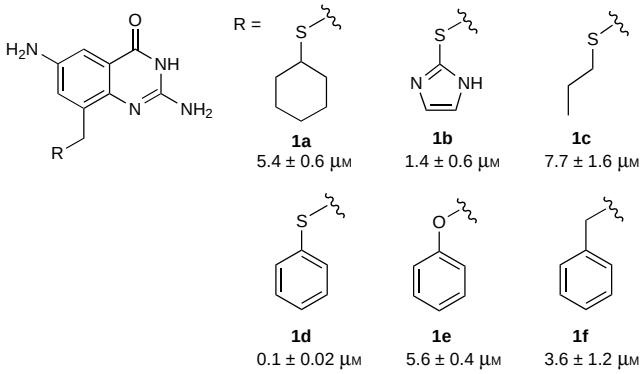


***Scheme 5.*** *Binding affinities ($K_i$ values, 37 °C) for inhibitors* ***1a–1f****.*

For the structural characterization of the complexes, TGT (*Z. mobilis*) was crystallized as described in ref. [19] and soaked with the inhibitors. X-ray crystal structures of the complexes formed by **1b** and **1c** were solved and nicely confirmed the inhibitor binding mode predicted at the design stage.[20] Figure 1a shows inhibitor **1c** complexed with TGT at a resolution of 1.8 Å; the complex of inhibitor **1b** at 1.7 Å resolution is shown from a different viewpoint in Figure 1b. Binding geometries are nearly identical in both complexes with the aminoquinazolinone moiety sandwiched between the side chains of Tyr106 and Met260. In both structures the Met260 S atom is located below the center of the heterocyclic ring of the quinazoline scaffold, with intermolecular distances to the six heavy atoms of this ring between 4.0 and 4.3 Å.[4, 14] As designed, the side chain at position 8 of the scaffold directs the thioimidazole ring (in **1b**) and the thiopropyl side chain (in **1c**) into the hydrophobic pocket defined by Leu68, Val45, and Val282. Both structures reveal crystallographic disorder about these molecular fragments, which perhaps indicates some additional space available in the hydrophobic pocket. Computer modeling suggests that

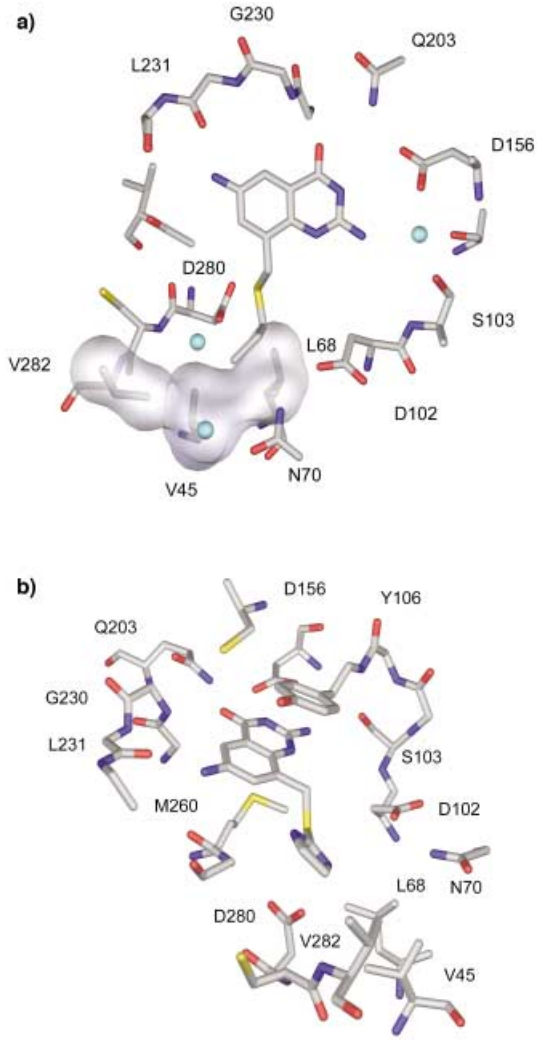


***Figure 1.*** *Experimentally determined structures of inhibitors* ***1 c*** *(a) and* ***1 b*** *(b) complexed at the active site of TGT (Z.* mobilis*) based on X-ray analysis. a) The binding of the thiopropyl side chain in* ***1 c*** *in the lipophilic pocket shown by its Connolly surface (blue spheres are isolated water molecules). b) The position of the aminoquinazolinone scaffold of* ***1 b*** *between Tyr106 and Met260 (water molecules are omitted). Hydrogen bonding patterns and distances are similar to those shown in Scheme 2. Color code: N: blue, O: red, S: yellow, C: grey.*

the other four inhibitors adopt similar binding geometries to those observed by the X-ray analysis of **1 b** and **1 c**, with their phenyl and cyclohexyl residues pointing into the lipophilic pocket.

The activity of the sulfur compound **1 d** ($K_i = 100$ nM) showed 56- and 36-fold enhancement in activity compared to its oxygen (**1 e**; $K_i = 5.6$ μM) and carbon (**1 f**; $K_i = 3.6$ μM) analogues. We rationalize these activity differences as a combination of hydrophobicity, electronic, and conformational effects. Differences in *c*log*P* values (a measure of hydrophobicity; *c* = concentration, *P* = partition function; **1 d**: 2.03; **1 e**: 1.47; **1 f**: 2.37)[21] point toward a reason for some of the binding difference between the O and S derivatives, since the latter clearly partitions more efficiently from the aqueous solution into the less polar enzyme active site. It is likely that the sulfur compound possesses a significantly different free energy of solvation since S atoms have less capacity to operate as hydrogen bond acceptors than O atoms. The side chain at position 8 of the inhibitor is transferred from an aqueous environment to a hydrophobic pocket which lacks direct hydrogen-bonding interactions with the ligand. Secondly, bonding of the S derivative **1 d** also benefits from the larger polarizability of sulfur compared to oxygen or carbon (S: 3.00 Å$^3$, O: 0.63 Å$^3$, $CH_2$: 1.80 Å$^3$),[22] which leads to stronger dispersion interactions. A search of related small-molecule structures within the Cambridge Structural Database (CSD)[23] was the basis for an evaluation of the structural and conformational differences between **1 d**–**f**. The phenyl rings of the three inhibitors should not all reach into the lipophilic pocket to the same depth, as predicted by their C–X bond lengths (C($sp^2$)–S: 1.77 Å, C($sp^2$)–O: 1.37 Å, C($sp^2$)–C: 1.51 Å). These differences are only partially compensated by the smaller C($sp^2$)–X–C($sp^3$) bond angle at sulfur (approximately 103° versus 118° for X = O and 113° for X = $CH_2$). Moreover, the CSD identifies a conformational preference of the thioanisole moiety in **1 d** which may also explain part of its superior inhibitory power compared to the equally lipophilic carbon derivative **1 f**. The dihedral angle C($sp^2$)$_{ortho}$–C($sp^2$)$_{ipso}$–X–C($sp^3$) required for the most favorable positioning of the phenyl ring in **1 d** (X = S) is about 0° (with a low calculated rotational energy barrier of roughly 5–6 kJ mol$^{-1}$ for the transition to the 90° arrangement).[24] While this is clearly also the favorable angle in **1 e** (X = O, rotational barrier of about 15 kJ mol$^{-1}$),[24] the optimal dihedral angle in **1 f** (X = $CH_2$) is approximately 90° (rotational barrier roughly 5 kJ mol$^{-1}$)[25] and thus a coplanar arrangement is less favorable in **1 f**.

The large S/O binding affinity difference was reproduced in two additional cases: upon replacement of the $NH_2$ group in position 6 of the quinazolinone scaffold in **1 d** and **1 e** by either a Br or an HO substituent (compounds and syntheses not shown). In the brominated series, the O derivative had $K_i = 11.9 \pm 2.2$ μM and the S derivative $K_i = 1.0 \pm 0.05$ μM, whereas in the hydroxylated series, the O derivative showed $K_i = 4.6 \pm 1.4$ μM and the S derivative $K_i = 250 \pm 50$ nM.

In conclusion, rational structure-based de novo design followed by convenient synthesis has provided a new class of inhibitors for prokaryotic TGT with promising biological activity. We have identified a new lipophilic pocket in the active site which opens up many avenues for further improvements of inhibitory affinity and selectivity. The molecular recognition properties of the pocket are still largely unexplored and are the target of current investigations. For example, the origins of the significant binding difference between cyclohexyl derivative **1 a** and its aromatic counterpart **1 d** have yet to be elucidated. Finally, we have demonstrated a remarkable "point mutation" effect on binding affinity in the context of $CH_2$ to O to S substitutions, a result which contributes to the general understanding of enzyme–inhibitor interactions.

*This work was supported by F. Hoffmann-La Roche, Basel, and the Deutsche Forschungsgemeinschaft (Grant KL-1204/1). R.K.C. is grateful to the U.S. National Science Foundation for an International Scholars Research postdoctoral fellowship. We thank Prof. K. Müller (F. Hoffmann-La Roche, Basel) for fruitful discussions*

 © WILEY-VCH-Verlag GmbH, 69451 Weinheim, Germany, 2002 1439-4227/02/03/02-03 $ 17.50+.50/0 ChemBioChem **2002**, No. 02-03

*concerning bonding interactions that involve sulfur, Dr. M. T. Stubbs for his help in the crystal structure determinations, and Prof. G. A. Garcia for providing samples of tRNA.*


[1] K. L. Kotloff, J. P. Winickoff, B. Ivanoff, J. D. Clemens, D. L. Swerdlow, P. J. Sansonetti, G. K. Adak, M. M. Levine, *Bull. World Health Organ.* **1999**, *77*, 651 – 666.

[2] W. A. Khan, C. Seas, U. Dahr, M. A. Salam, M. L. Bennish, *Ann. Intern. Med.* **1997**, *126*, 697 – 703.

[3] M. L. Cohen, *Nature* **2000**, *406*, 762 – 767.

[4] U. Grädler, H.-D. Gerber, D. M. Goodenough-Lashua, G. A. Garcia, R. Ficner, K. Reuter, M. T. Stubbs, G. Klebe, *J. Mol. Biol.* **2001**, *306*, 455 – 467.

[5] R. K. Slany, H. Kersten, *Biochimie* **1994**, *76*, 1178 – 1182.

[6] N. Okada, S. Nishimura, *J. Biol. Chem.* **1979**, *254*, 3061 – 3066.

[7] N. Okada, S. Noguchi, H. Kasai, N. Shindo-Okada, T. Oghi, T. Goto, S. Nishimura, *J. Biol. Chem.* **1979**, *254*, 3067 – 3073.

[8] R. C. Morris, K. G. Brown, M. S. Elliott, *J. Biomol. Struct. Dyn.* **1999**, *16*, 757 – 774.

[9] J. M. B. Durand, B. Dagberg, B. E. Uhlin, G. R. Björk, *Mol. Microbiol.* **2000**, *35*, 924 – 935.

[10] a) U. Obst, V. Gramlich, F. Diederich, L. Weber, D. W. Banner, *Angew. Chem.* **1995**, *107*, 1874 – 1877; *Angew. Chem. Int. Ed. Engl.* **1995**, *34*, 1739 – 1742; b) U. Obst, P. Betschmann, C. Lerner, P. Seiler, F. Diederich, V. Gramlich, L. Weber, D. W. Banner, P. Schönholzer, *Helv. Chim. Acta* **2000**, *83*, 855 – 909.

[11] a) B. Masjost, P. Ballmer, E. Borroni, G. Zürcher, F. K. Winkler, R. Jakob-Roetne, F. Diederich, *Chem. Eur. J.* **2000**, *6*, 971 – 982; b) C. Lerner, A. Ruf, V. Gramlich, B. Masjost, G. Zürcher, R. Jakob-Roetne, E. Borroni, F. Diederich, *Angew. Chem.* **2001**, *113*, 4164 – 4166; *Angew. Chem. Int. Ed.* **2001**, *40*, 4040 – 4042.

[12] C. Romier, K. Reuter, D. Suck, R. Ficner, *EMBO J.* **1996**, *15*, 2850 – 2857. The residues that participate in substrate binding and catalysis of *Z. mobilis* TGT are identical to those of the *Shigella flexneri* enzyme, apart from the replacement of Tyr106 by Phe.

[13] P. R. Gerber, K. Müller, *J. Comput.-Aided Mol. Design* **1995**, *9*, 251 – 268.

[14] R. J. Zauhar, C. L. Colbert, R. S. Morgan, W. J. Welsh, *Biopolymers* **2000**, *53*, 233 – 248.

[15] D. J. McNamara, E. M. Berman, D. W. Fry, L. M. Werbel, *J. Med. Chem.* **1990**, *33*, 2045 – 2051.

[16] J. Yin, C. Pidgeon, *Tetrahedron Lett.* **1997**, *38*, 5953 – 5954.

[17] H.-J. Hess, T. H. Cronin, A. Scriabine, *J. Med. Chem.* **1968**, *11*, 130 – 138.

[18] E. C. Taylor, C. Yoon, *Synth. Commun.* **1988**, *18*, 1187 – 1191.

[19] C. Romier, R. Ficner, K. Reuter, D. Suck, *Proteins: Struct. Funct. Genet.* **1996**, *24*, 516 – 519.

[20] X-ray data for the TGT inhibitor complexes were collected to a resolution of 1.70 Å and a completeness of 99.5 % (**1b**) and to a resolution of 1.80 Å and a completeness of 99.6 % (**1c**). Phases were calculated by using protein and water coordinates from TGT (*Z. mobilis*; Protein Databank (PDB) code: 1ENU). The protein and inhibitor structures were refined (A. T. Brünger, X-PLOR, Version 3.1, Yale University Press, New Haven, **1992**) and yielded an *R* value of 19.9 % ($R_{free}$ of 24.1 %) for 406 718 reflections for **1b** (44 700 unique reflections; standard deviation for bond lengths of 0.006 Å and for bond angles of 1.367 Å) and an *R* value of 19.6 % ($R_{free}$ of 22.9 %) for 351 534 reflections for **1c** (38 143 unique reflections; standard deviation for bond lengths of 0.005 Å and for bond angles of 1.278 Å). Coordinates of the TGT – **1b** and TGT – **1c** complexes have been deposited in the RCSB Protein Databank with the PDB codes 1K4G and 1K4H, respectively.

[21] clog*P* Values were calculated by using SPARTAN v. 5.1.3 (Wavefunction, Inc., Irvine, **1998**) and the Ghose parameters.

[22] A. R. Fersht, C. Dingwall, *Biochemistry* **1979**, *18*, 1245 – 1249.

[23] CSD System, Version 5.21, April 2001 release, as implemented through ConQuest. See: *http://www.ccdc.cam.ac.uk* for details.

[24] T. Schaefer, R. Sebastian, S. R. Salman, J. D. Baleja, G. H. Penner, D. M. McKinnon, *Can. J. Chem.* **1991**, *69*, 620 – 624, and references cited therein.

[25] T. Schaefer, P. Hazendonk, D. M. McKinnon, *Can. J. Chem.* **1995**, *73*, 1387 – 1394.


Received: October 17, 2001 [Z307]

# Synthesis and Characterisation of Acyl Carrier Protein Bound Polyketide Analogues

Christopher Arthur, Russell J. Cox,* John Crosby, Mujiber M. Rahman, Thomas J. Simpson, Florilene Soulas, Roberto Spogli, Anna E. Szafranska, James Westcott, and Christopher J. Winfield[a]

**KEYWORDS:**

acyl carrier protein · biosynthesis · intermediates · polyketides

Polyketide synthases (PKSs) are widespread in plants, bacteria and fungi.[1] They are responsible for the biosynthesis of an enormous range of organic compounds, many of which have important pharmaceutical and agrochemical properties.[2] Three types of synthases have been documented. Type I systems consist of very large multifunctional proteins which can be either processive (for example the modular systems responsible for macrolide synthesis)[3] or iterative (for example the lovastatin nonaketide synthase from *Aspergillus terreus*[4]). The iterative Type II PKS systems consist of complexes of monofunctional proteins exemplified by the actinorhodin (act) **1** PKS from *Streptomyces coelicolor*.[5] Type III systems are responsible for the synthesis of chalcones and stilbenes in plants and polyhydroxy phenols in bacteria.[6] All PKS possess the key $\beta$-ketoacyl synthase domain responsible for the C—C bond forming reaction. In Type I and Type II systems the growing acyl chain is covalently attached to the terminal thiol of a phosphopantetheine (PP) prosthetic group on an acyl carrier protein (ACP).

In the act PKS a minimal set of proteins has been identified which is capable of synthesising polyketides in vitro from malonyl CoA.[7] These proteins are $KS_\alpha$, responsible for C—C bond formation, $KS_\beta$ responsible inter alia for starter unit production[8] and the ACP (Figure 1).[9] We have extensively studied these components and their biochemical activities in vitro. In short, these proteins load malonyl units onto the terminal PP thiol of the ACP (Scheme 1).[10] $KS_\beta$ then produces acetyl-ACP and $KS_\alpha$ performs seven decarboxylative condensations to produce a putative ACP-bound octaketide. The subsequent cyclisation and release of this octaketide, probably controlled by the minimal PKS, yields SEK4 (**2**) and SEK4b (**3**) as the products.

We studied the acyl ACP intermediates formed during PKS catalysis. Novel acyl ACPs could act as surrogate intermediates or starter units for PKS and may lead to the synthesis of novel compounds in vitro. Acyl ACPs could also be substrates for other

[a] *Dr. R. J. Cox, C. Arthur, Dr. J. Crosby, M. M. Rahman, Prof. T. J. Simpson FRS, F. Soulas, R. Spogli, A. E. Szafranska, J. Westcott, Dr. C. J. Winfield*
*School of Chemistry*
*University of Bristol*
*Cantock's Close, Clifton*
*Bristol, BS8 1AS (UK)*
*Fax: (+44) 117-929-8611*
*E-mail: r.j.cox@bris.ac.uk*